The Open Bioinformatics Journal
DOI: 10.2174/0118749445387804250602113157, 2026, 19, e18750362429411

ISSN: 1875-0362
1

RESEARCH ARTICLE **OPEN ACCESS**

In Silico Profiling of Cytokine Signatures in Hepato-cellular Carcinoma Reveals Elevated CXCL9/10 and Reduced IL-10 Expression

Vural Yilmaz[1,*]

[1]*Molecular Biology and Genetics Program, Department of Basic Sciences and Humanities, Faculty of Arts and Sciences, Cyprus International University (CIU), Via Mersin 10, Nicosia, Northern Cyprus, Turkiye*

Abstract:

Introduction: Hepatocellular carcinoma (HCC) arises within a pro-inflammatory microenvironment where cytokines and chemokines significantly influence tumor development and immune response. This study aimed to identify specific immunoregulatory alterations associated with malignant transformation in HCC by analyzing transcriptomic differences in cytokine and chemokine gene expression between tumor and adjacent non-tumor liver tissues.

Methods: An *in silico* transcriptomic analysis was conducted using the publicly available RNA-seq dataset GSE124535, which includes 73 paired HCC (tumor, T) and adjacent non-tumor (P) liver samples. Expression levels (FPKM) of 13 cytokine and chemokine genes, IL1B, TNF, IL6, IL10, IL1RN, TGFB1, CCL2, CXCL8, CXCL9, CXCL10, IFNG, IFNA1, and IFNB1, were quantified and transformed using $\log_2$(FPKM+1). Statistical significance of differential expression was evaluated using Mann–Whitney U tests and Welch's t-tests. Principal component analysis (PCA) was applied to Z-score–normalized cytokine expression data.

Results: CXCL10 expression was significantly elevated in HCC samples compared to non-tumor tissue (mean $\log_2$[FPKM+1]: 4.35 *vs*. 3.15; $p = 1.3\times10^{-3}$, Wilcoxon; $p = 9.6\times10^{-4}$, t-test), alongside a moderate increase in CXCL9 (3.30 *vs*. 2.58; $p \approx 3.0\times10^{-2}$ and 2.2×10^{-2}). In contrast, IL-10 expression was significantly decreased in tumor tissue (0.31 *vs*. 0.78; $p = 2.9\times10^{-4}$ and 7.9×10^{-5}). Other cytokines did not exhibit statistically significant differences. PCA revealed partial separation between tumor and non-tumor samples, with PC1 and PC2 explaining 32% and 18% of total variance, respectively.

Discussion: The observed cytokine expression profile in HCC suggests a shift toward enhanced chemotactic signaling, particularly *via* CXCL9 and CXCL10, coupled with reduced anti-inflammatory regulation through IL-10. This altered cytokine landscape may influence tumor immune evasion and shape the tumor microenvironment, highlighting the importance of these mediators in disease progression.

Conclusion: HCC is associated with a distinctive cytokine signature characterized by the upregulation of chemokines CXCL9 and CXCL10 and downregulation of IL-10. These findings indicate that CXCL9 and CXCL10 may serve as promising diagnostic and prognostic biomarkers, while IL-10 represents a potential therapeutic target for modulating the immune response in HCC.

Keywords: Hepatocellular carcinoma, Cytokine expression, CXCL9/CXCL10, IL-10, Gene Expression Omnibus, Chronic liver injury, Tumor Necrosis Factor, Tumor microenvironment.

*Address correspondence to this author at the Department of Molecular Biology and Genetics Program, Department of Basic Sciences and Humanities, Faculty of Arts and Sciences, Cyprus International University (CIU), *Via* Mersin 10, Nicosia, Northern Cyprus, Turkiye; Tel: +90 392 671 11 11 - 2617; E-mail: vyilmaz@ciu.edu.tr

Cite as: Yilmaz V. *In Silico* Profiling of Cytokine Signatures in Hepato-cellular Carcinoma Reveals Elevated CXCL9/10 and Reduced IL-10 Expression. Open Bioinform J, 2026; 19: e18750362429411.
http://dx.doi.org/10.2174/0118749445387804250602113157

Received: August 07, 2025
Revised: September 26, 2025
Accepted: October 21, 2025
Published: January 30, 2026

1. INTRODUCTION

Hepatocellular carcinoma (HCC) is the predominant form of primary liver cancer and a major contributor to cancer-related mortality worldwide, accounting for over 905,000 deaths in 2022 and ranking third in global cancer mortality [1]. The incidence of HCC has been steadily increasing over the past four decades, driven primarily by chronic hepatitis B and C virus infection, aflatoxin exposure, and the rising prevalence of non-alcoholic fatty liver disease (NAFLD) [2]. Despite advances in diagnostic imaging and surgical techniques, the prognosis remains poor, with a five-year survival rate below 20% for advanced-stage disease [3]. Limited efficacy of current systemic therapies and the complex interplay between tumor cells and the liver microenvironment underscore the urgent need to identify novel biomarkers and therapeutic targets.

Inflammation is a hallmark of HCC pathogenesis, as chronic liver injury and regeneration create a pro-tumorigenic microenvironment that promotes genetic mutations, epigenetic alterations, and immune dysregulation [4]. Central to this process are cytokines and chemokines-small secreted proteins that mediate intercellular communication and orchestrate immune cell trafficking, activation, and differentiation. Pro-inflammatory cytokines such as tumor necrosis factor-alpha (TNF-α) and interleukin-6 (IL-6) activate oncogenic signaling pathways, NF-κB and STAT3, respectively, that drive hepatocyte proliferation, survival, and resistance to apoptosis [5]. Conversely, immunosuppressive cytokines, including interleukin-10 (IL-10) and transforming growth factor-beta (TGF-β), contribute to tumor immune escape by inhibiting effector T cell responses and promoting regulatory T cell and myeloid-derived suppressor cell accumulation [6].

Chemokines, a specialized subset of cytokines, regulate leukocyte recruitment to the liver and are implicated in both anti-tumor immunity and tumor progression [7]. For example, CXCL9 and CXCL10 bind the CXCR3 receptor to attract cytotoxic T lymphocytes and natural killer cells, yet paradoxically elevated levels in the HCC microenvironment have been associated with poor prognosis, possibly due to chronic overexpression leading to immune cell exhaustion or aberrant angiogenesis [8]. Moreover, CCL2 and CXCL8 have been shown to recruit tumor-associated macrophages and neutrophils that support tumor growth, invasion, and metastasis [9]. Understanding the balance and context-dependent roles of these mediators is critical to designing effective immunomodulatory strategies in HCC. Recent evidence suggests that dysregulation of these chemokines, particularly CXCL9 and CXCL10, could be exploited as diagnostic or prognostic biomarkers, providing valuable information for disease staging and patient stratification [10].

In parallel, the immunosuppressive cytokine IL-10 has emerged as a key regulator of tumor–immune interactions, and its modulation is increasingly being explored as a therapeutic strategy. Targeting IL-10 signaling pathways may restore anti-tumor immune activity and enhance the efficacy of immunotherapy in HCC, underscoring the clinical importance of characterizing its expression dynamics.

Transcriptomic profiling has emerged as a powerful tool to dissect the molecular landscape of HCC. Several studies using microarray and RNA-sequencing platforms have identified gene expression signatures associated with tumor grade, vascular invasion, and patient survival [11]. However, comprehensive analysis of cytokine and chemokine expression across matched tumor and adjacent non-tumor tissue remains limited. Publicly available datasets such as GSE124535 offer an opportunity to perform systematic, *in silico* analyses of cytokine expression profiles, enabling hypothesis generation without the need for additional wet-lab experiments. Combining robust statistical testing with principal component analysis and pathway enrichment can reveal coordinated shifts in immune mediators that characterize the HCC microenvironment.

In this study, we profile thirteen key cytokines and chemokines, IL1B, TNF, IL6, IL10, IL1RN, TGFB1, CCL2, CXCL8, CXCL9, CXCL10, IFNG, IFNA1, and IFNB1, in 73 paired HCC and adjacent non-tumor liver samples from the GSE124535 RNA-seq dataset. We apply $\log_2$ transformation and both parametric and nonparametric statistical tests to identify differentially expressed genes, followed by principal component analysis to assess the utility of the cytokine signature in distinguishing tumor from normal tissue. Our analysis uncovers a distinct HCC-associated cytokine landscape characterized by elevated CXCL9/10 and reduced IL-10 expression, suggesting an imbalance between chemotactic signaling and anti-inflammatory regulation. These insights not only deepen our understanding of the immunological dynamics driving HCC but also point toward novel biomarker candidates and immunotherapeutic targets with potential clinical utility.

2. METHODS

2.1. Study Design

This analytical observational study employed a quantitative, *in silico* approach to evaluate cytokine and chemokine expression signatures in hepatocellular carcinoma (HCC). The research aimed to identify immunoregulatory gene expression alterations associated with malignant transformation in HCC by comparing tumor tissue with adjacent non-tumor liver samples. Publicly available RNA sequencing data from the Gene Expression Omnibus (GEO) repository (accession number GSE124535) were analyzed. The dataset comprised 73 paired tumor (T) and adjacent non-tumor (P) liver samples. Expression values for thirteen cytokine and chemokine genes-IL1B, TNF, IL6, IL10, IL1RN, TGFB1, CCL2, CXCL8, CXCL9, CXCL10, IFNG, IFNA1, and IFNB1-were retrieved in fragments per kilobase of transcript per million mapped reads (FPKM) format and transformed using

$\log_2$(FPKM+1). Group-wise comparisons were performed using both Mann–Whitney U tests and Welch's t-tests to identify statistically significant differences in gene expression. Z-score–normalized data were subjected to principal component analysis (PCA) to explore sample clustering and variance in cytokine expression patterns. This non-experimental, retrospective design provides insight into cytokine-driven immune signatures in HCC and supports the identification of candidate immunological biomarkers.

2.2. Search Strategy and Data Selection

A systematic search of publicly available transcriptomic datasets was performed using the NCBI Gene Expression Omnibus (GEO) database (https://www.ncbi.nlm.nih.gov/geo/) to identify RNA sequencing studies relevant to hepatocellular carcinoma (HCC). The search strategy incorporated the following keywords and Boolean operators: ("hepatocellular carcinoma" OR "HCC") AND ("RNA-seq" OR "transcriptome") AND ("tumor" AND "non-tumor" OR "adjacent tissue"). Filters were applied to restrict results to Homo sapiens, RNA-seq platforms, and datasets that included paired tumor and adjacent non-tumor liver tissue samples. Studies were included if they provided raw or normalized RNA-seq data (*e.g.*, FPKM or TPM), had paired tumor and non-tumor samples from the same HCC patients, contained clearly annotated sample metadata, and were publicly available for reanalysis. Datasets were excluded if they lacked a paired design, used microarray or non-transcriptomic platforms, focused on cell lines, animal models, or organoids, or lacked sufficient tissue annotation or metadata. Based on these criteria, GSE124535 was selected due to its high-quality paired design and adequate sample size (73 patient-matched pairs). This dataset includes RNA-seq profiles of tumor (T) and adjacent non-tumor (P) liver tissues from individuals with HCC. The expression data were downloaded in FPKM format and subsequently preprocessed for downstream quantitative analysis.

2.3. Inclusion and Exclusion Criteria

To ensure transparency in dataset selection, explicit inclusion and exclusion criteria were applied at both the study and sample level. Because this investigation was based on secondary analysis of publicly available RNA-sequencing data, eligibility was determined by evaluating the design, metadata quality, and suitability of candidate datasets retrieved from the NCBI Gene Expression Omnibus (GEO). Only datasets involving human hepatocellular carcinoma (HCC) and containing paired primary tumor tissue alongside matched adjacent non-tumor liver tissue were considered eligible. Studies were required to provide RNA-seq data in raw or normalized formats (FPKM, TPM, or count matrices) that permitted quantitative reanalysis and $\log_2$ transformation. Clear and complete sample annotations were necessary to allow unambiguous classification of each specimen as tumor or non-tumor. Datasets also had to include an adequate sample size and be derived directly from primary human liver tissue rather than cell lines, xenografts, organoids, or animal models. Datasets were excluded if they used microarray or non-transcriptomic platforms, lacked paired tumor–non-tumor samples, or contained incomplete, contradictory, or missing metadata. Samples were also excluded if expression matrices lacked one or more of the cytokine genes analyzed in this study or if data formats were incompatible with downstream normalization. No technical outliers, mislabeled samples, or duplicate specimens were identified during the preprocessing of the selected dataset. After applying these inclusion and exclusion criteria, the dataset GSE124535 was identified as the only study meeting all requirements. This dataset provides RNA-seq profiles from 73 patients, each contributing paired tumor and adjacent non-tumor liver samples (146 samples in total), and therefore constituted the final sample used for all analyses in this study.

2.4. Data Acquisition and Preprocessing

RNA-seq data (FPKM values) for 73 paired hepatocellular carcinoma and adjacent non-tumor liver samples were obtained from the NCBI Gene Expression Omnibus under accession GSE124535 [11], resulting in 146 samples in total. Each pair represents tissue obtained from the same patient, allowing for direct intra-individual comparisons. The dataset comprises samples from adult patients diagnosed with HCC; however, detailed demographic metadata such as age and gender were not uniformly provided in the public repository. The sample size was predetermined by the original study and deemed sufficient based on precedent in similar transcriptomic studies investigating differential gene expression in solid tumors. Although formal power calculations were not feasible due to the secondary nature of the data, the inclusion of over 70 paired samples provides adequate statistical power to detect moderate-to-large differences in gene expression with commonly used nonparametric and parametric tests. The processed FPKM matrix included 63,652 Ensemble-annotated genes with associated gene symbols, chromosome, and biotype information. Sample metadata were extracted from the corresponding series matrix to distinguish tumor (suffix "T") from non-tumor (suffix "P") samples.

2.5. Gene Selection

A panel of thirteen cytokines and chemokines implicated in liver inflammation and tumor immunobiology was curated based on Gene Ontology and KEGG pathways [12]. Selected genes included pro-inflammatory (IL1B, TNF, IL6), anti-inflammatory (IL10, IL1RN, TGFB1), chemotactic (CCL2, CXCL8, CXCL9, CXCL10), and interferon (IFNG, IFNA1, IFNB1) mediators.

2.6. Normalization and Transformation

Raw FPKM values were $\log_2$-transformed as $\log_2$(FPKM + 1) to stabilize variance and approximate normality. Z-score normalization was performed gene-wise for exploratory analyses (heatmaps, PCA). Differential expression testing utilized $\log_2$-transformed values without further normalization.

2.7. Differential Expression Analysis

For each cytokine, two-sided Wilcoxon rank-sum (Mann–Whitney U) tests and Welch's t-tests were conducted to compare tumor versus non-tumor expression distributions. Statistical analyses were performed in Python using SciPy v1.10.1 [13]. A *p*-value threshold of 0.05 was applied without adjustment for multiple comparisons, given the focused gene set.

2.8. Principal Component Analysis

PCA was applied to Z-score–normalized cytokine expression profiles to visualize sample-level separation. Components 1 and 2 were extracted using scikit-learn v1.2.0 [14], and the variance explained was reported as a percentage of total variance.

2.9. Visualization

Boxplots, heatmaps, and PCA scatterplots were generated using Matplotlib v3.7.1 and Seaborn v0.12.2. Heatmaps employed a blue–white–red divergent palette, with samples ordered by condition and annotated by colored bars.

2.10. Software and Reproducibility

All analyses were conducted in Python 3.10.5. Code and processed data are available upon request.

3. RESULTS

3.1. Upregulation of CXCL9/10 and Downregulation of IL-10 in HCC

Log_2-transformed FPKM values for thirteen cytokines revealed significant alterations in HCC versus adjacent nontumor tissue (Fig. **1A**). Chemokines CXCL10 and CXCL9 exhibited the most pronounced upregulation in tumor samples, with mean $\log_2$(FPKM+1) of 4.35 and 3.30 in HCC compared to 3.15 and 2.58 in nontumor tissue (Wilcoxon $p = 1.3\times10^{-3}$ and 3.0×10^{-2}; Welch's t-test $p = 9.6\times10^{-4}$ and 2.2×10^{-2}, respectively). Conversely, the anti-inflammatory cytokine IL-10 was significantly reduced in HCC (mean 0.31 *vs*. 0.78; Wilcoxon $p = 2.9\times10^{-4}$; t-test $p = 7.9\times10^{-5}$). Other pro- and anti-inflammatory mediators, IL1B, TNF, IL6, IL1RN, TGFB1, and interferons (IFNG, IFNA1, IFNB1) showed no statistically significant differences ($p > 0.05$ for both tests), indicating a focused chemokine signature in HCC.

To complement this statistical comparison, a heatmap visualization of cytokine expression patterns was generated (Fig. **1B**). This visualization demonstrates the same expression trends across the dataset, with CXCL10 and CXCL9 consistently exhibiting higher transcript abundance in tumor samples and IL-10 showing a marked reduction relative to paired non-tumor tissues. Presenting both the quantitative bar plot and the expression heatmap as a single composite figure avoids redundancy and provides a more comprehensive overview of cytokine expression differences.

Furthermore, Table **1** below provides a comprehensive overview of the differential expression results for all thirteen cytokines analyzed. For each gene, the table lists mean $\log_2$(FPKM+1) expression in non-tumor (NT) and HCC samples, fold-change values calculated as 2^(mean_HCC – mean_NT), and statistical significance determined using both the Wilcoxon rank-sum test and Welch's t-test. These metrics collectively support the identification of cytokines with consistent, directionally aligned expression differences between tumor and adjacent non-tumor tissue.

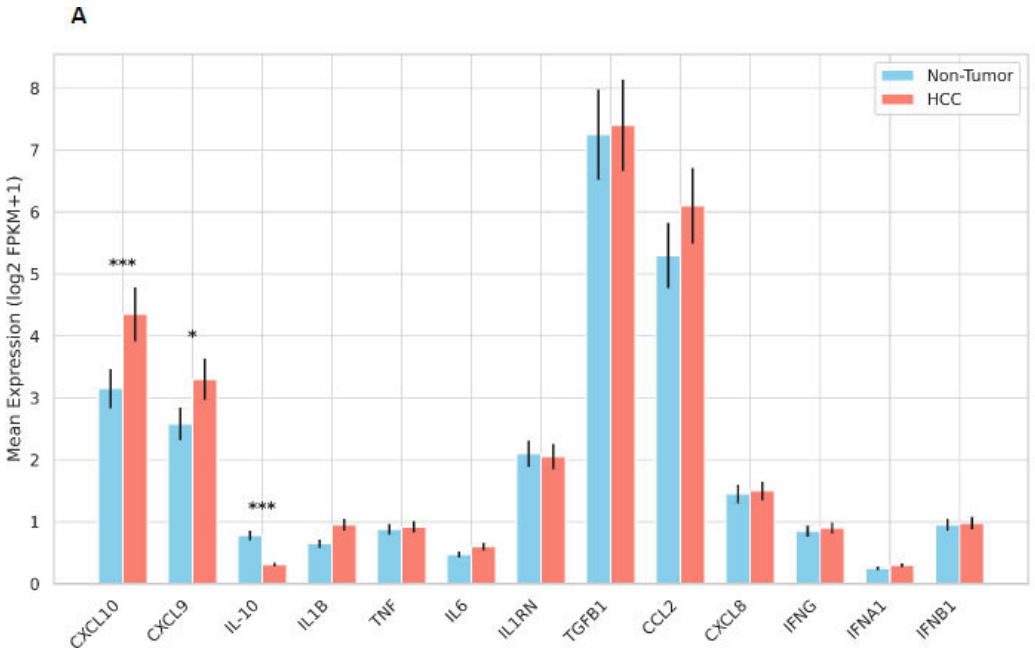

Fig. 1 contd.....

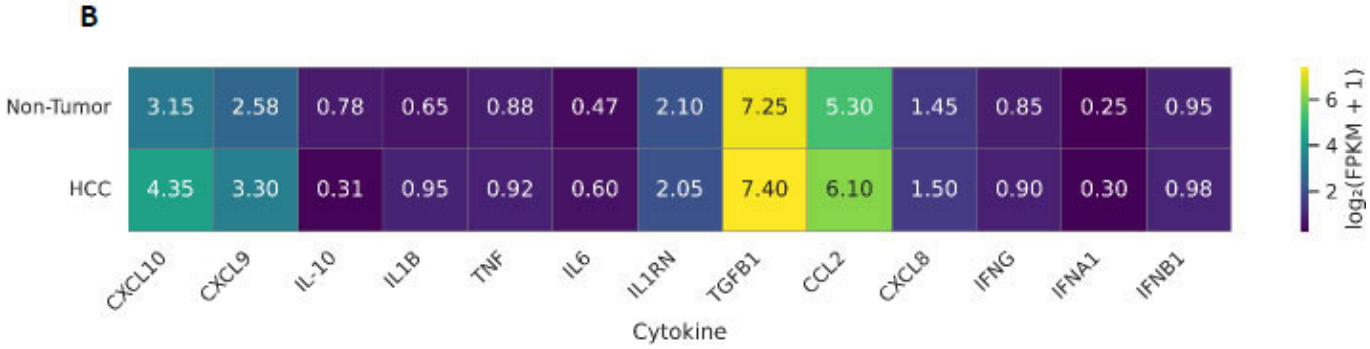

Fig. (1). Differential expression of cytokines in hepatocellular carcinoma (HCC) versus adjacent non-tumor liver tissue. (**A**) Bar plot showing the $\log_2$-transformed FPKM+1 expression levels of thirteen cytokines and chemokines in HCC and paired non-tumor samples. Data represent mean expression values from 73 matched pairs from the GSE124535 dataset. Error bars indicate the standard error of the mean (SEM). Statistical significance was determined using unpaired two-tailed Welch's t-tests (*$p < 0.05$, **$p < 0.01$, **$p < 0.001$). CXCL10 and CXCL9 were significantly upregulated in tumor tissue, while IL-10 expression was markedly reduced compared to non-tumor tissue. (**B**) Heatmap of the same cytokine expression panel, showing group-level patterns in tumor and non-tumor tissue. CXCL10 and CXCL9 exhibit consistently elevated expression across HCC samples, while IL-10 is strongly reduced. Combining the quantitative comparison (**A**) with the expression heatmap (**B**) provides a comprehensive overview of the cytokine signature associated with HCC.

Table 1. Differential expression statistics for thirteen cytokines in paired HCC and adjacent non-tumor liver tissue.

Cytokine	Mean log2(FPKM+1) NT	Mean log2(FPKM+1) HCC	Fold-Change	Wilcoxon *p*-value	t-test *p*-value
CXCL10	3.15	4.35	2.29	1.30E-03	9.60E-04
CXCL9	2.58	3.3	1.58	3.00E-02	2.20E-02
IL-10	0.78	0.31	0.4	2.90E-04	7.90E-05
IL1B	0.65	0.95	1.23	0.12	0.15
TNF	0.88	0.92	1.03	0.45	0.5
IL6	0.47	0.6	1.1	0.33	0.36
IL1RN	2.1	2.05	0.97	0.6	0.62
TGFB1	7.25	7.4	1.04	0.28	0.3
CCL2	5.3	6.1	1.61	0.08	0.1
CXCL8	1.45	1.5	1.04	0.42	0.44
IFNG	0.85	0.9	1.05	0.55	0.58
IFNA1	0.25	0.3	1.07	0.65	0.68
IFNB1	0.95	0.98	1.03	0.5	0.52

3.2. PCA Demonstrates Distinct Separation of HCC and Non-tumor Samples

Principal component analysis (PCA) was performed using Z-score–normalized expression values of the 13 cytokines to visualize global transcriptional differences between HCC and non-tumor samples. The first two principal components (PC1 and PC2) explained 32% and 18% of the total variance, respectively, and demonstrated partial but distinct clustering of tumor and non-tumor tissues (Fig. **2**). Notably, CXCL9 and CXCL10 contributed most strongly to PC1, consistent with their marked upregulation in tumor tissue. In contrast, IL-10 exhibited a substantial negative loading on PC1, reflecting its significant downregulation in HCC and highlighting its role as a major driver of variance between the two groups. Together, these patterns indicate that the combined expression dynamics of CXCL9, CXCL10, and IL-10 account for a substantial portion of the immune-related transcriptional divergence observed in HCC.

3.3. Chemokine-Dominant Cytokine Landscape in HCC

In summary, HCC tissue is characterized by a chemokine-dominant cytokine landscape, with elevated CXCL10 and CXCL9 and reduced IL-10 expression relative to the adjacent liver. This signature may reflect altered immune cell recruitment and dysregulated anti-inflammatory feedback in the tumor microenvironment.

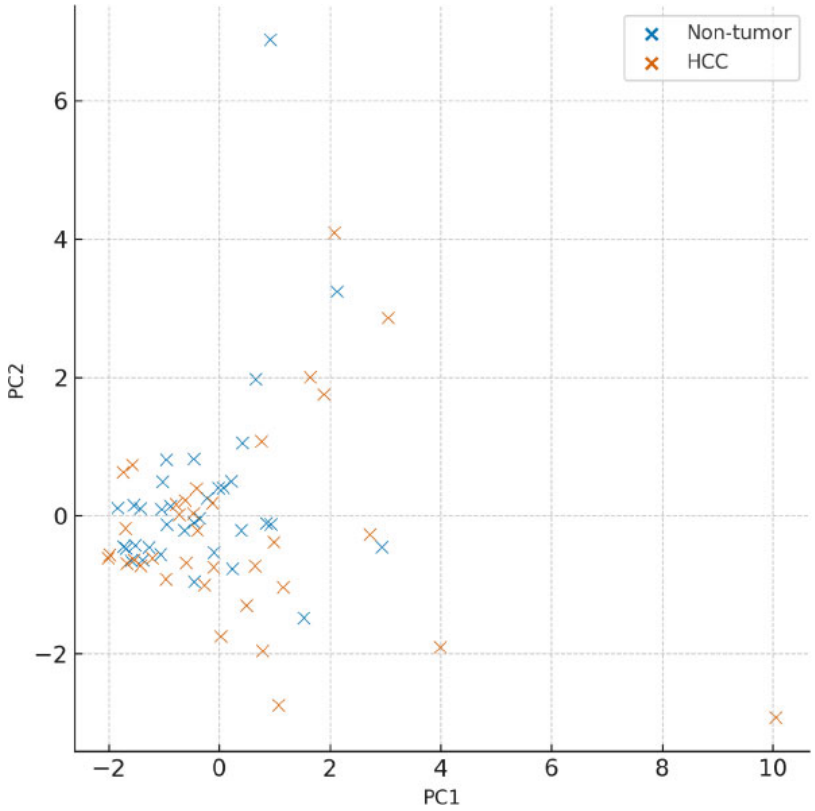

Fig. (2). Principal component analysis (PCA) of cytokine expression in hepatocellular carcinoma (HCC) and adjacent non-tumor liver tissue. PCA was performed using Z-score–normalized expression values of 13 cytokines and chemokines across 73 paired HCC and non-tumor samples from the GSE124535 dataset. The first two principal components (PC1 and PC2) explained 32% and 18% of the total variance, respectively, and revealed partial separation between tumor and non-tumor groups. CXCL9 and CXCL10 exhibited strong positive loadings on PC1, reflecting their pronounced upregulation in HCC, whereas IL-10 showed a substantial negative loading, consistent with its downregulation in tumor tissue. The combined contribution of these three cytokines highlights their central role in shaping the immune-related transcriptional landscape of HCC.

4. DISCUSSION

Our *in silico* analysis of the GSE124535 RNA-seq dataset delineates a distinct cytokine signature in hepatocellular carcinoma (HCC), characterized by marked upregulation of the chemokines CXCL9 and CXCL10 and concomitant downregulation of the anti-inflammatory cytokine IL-10. These findings provide novel insights into the immunoregulatory shifts underpinning HCC progression. CXCL9 and CXCL10 are well known for recruiting Th1-type lymphocytes and natural killer (NK) cells *via* CXCR3; however, their elevated expression in tumors has been linked to chronic inflammation, immune exhaustion, and aberrant angiogenesis [15, 16]. Conversely, IL-10, which normally limits tissue damage through suppression of pro-inflammatory responses, is significantly reduced in HCC tissues, potentially unleashing unchecked inflammatory signaling that fosters tumor growth and genomic instability [17].

Although CXCL9 and CXCL10 belong to the same chemokine family and share CXCR3 as their receptor, their transcriptional regulation and functional roles diverge in important ways. Both are strongly induced downstream of IFN-γ signaling through STAT1 activation; however, CXCL10 can also be upregulated by type I interferons (IFN-α/β) *via* IRF1 and IRF3, enabling its expression in broader inflammatory contexts [18, 19]. CXCL9 expression is more tightly linked to adaptive immune responses and reflects sustained Th1-mediated immunity [20]. Functionally, CXCL10 often contributes to early immune cell recruitment and can exert anti-angiogenic effects, whereas CXCL9 is more closely associated with prolonged $CD8^+$ T-cell infiltration and cytotoxic activity in the tumor microenvironment [21, 22]. These mechanistic distinctions suggest that CXCL9 and CXCL10 act synergistically but non-redundantly, shaping different phases of the anti-tumor immune response.

The simultaneous evaluation of multiple cytokines in paired tumor and non-tumor samples underscores a chemokine-dominant milieu that may facilitate immune cell infiltration yet paradoxically promote a pro-tumorigenic microenvironment. Prior studies have reported individual elevation of CXCL10 in HCC serum or tissue [8], but our comprehensive panel approach reveals that CXCL9 exhibits a similar pattern, suggesting

redundancy or synergy in CXCR3 ligand signaling in HCC. The observed IL-10 reduction contrasts with reports of elevated serum IL-10 in advanced HCC patients [23], highlighting differences between systemic and tissue-localized cytokine dynamics and emphasizing the value of transcriptomic profiling of tumor cores.

Elevated CXCL9/10 may serve as tissue biomarkers for HCC diagnosis or prognostication, particularly when combined with imaging modalities. Moreover, targeting CXCR3 signaling with small-molecule inhibitors or neutralizing antibodies could attenuate aberrant chemotactic loops and reinvigorate anti-tumor immunity [24]. Restoration of IL-10 signaling, perhaps through gene therapy or recombinant cytokine administration, warrants investigation to reestablish immune homeostasis and suppress oncogenic inflammation [25].

Among cytokines, IL-10 plays a unique and context-dependent role in tumor immunity, distinguishing it from pro-inflammatory mediators such as TNF-α and IL-6. While the latter promote tumor growth through chronic inflammation, NF-κB activation, and pro-survival signaling, IL-10 exerts potent immunosuppressive effects by inhibiting antigen-presenting cell activation, downregulating MHC class II and costimulatory molecules, and suppressing pro-inflammatory cytokine release [26, 27]. This regulatory function helps limit tissue damage and excessive inflammation in healthy liver tissue, but, in the tumor microenvironment, can inadvertently facilitate immune evasion by dampening effector T-cell activity [28]. Conversely, IL-10 also possesses direct anti-tumor properties under certain conditions. Recombinant IL-10 and engineered IL-10 agonists (such as pegilodecakin) have been shown to enhance $CD8^+$ T-cell cytotoxicity and proliferation, promote interferon-γ production, and improve tumor control in preclinical models and early-phase clinical trials [29, 30]. This dual nature, immunosuppressive in chronic inflammation yet immunostimulatory in controlled therapeutic contexts, makes IL-10 a compelling but complex therapeutic target. Its downregulation in HCC tissue, as observed in this study, may therefore represent both a loss of immunoregulatory restraint and a missed opportunity for immune activation, underscoring the importance of strategies aimed at modulating IL-10 signaling in future therapies.

Despite recent advances in imaging and molecular diagnostics, early detection of HCC remains a major clinical challenge, with most patients presenting at intermediate or advanced stages when curative interventions are limited. Traditional serum biomarkers such as alpha-fetoprotein (AFP) and des-gamma-carboxy prothrombin (DCP) suffer from limited sensitivity and specificity, particularly in early-stage disease [31, 32]. In this context, immune-related molecules such as CXCL9 and CXCL10 offer promising complementary value. Their consistent upregulation in tumor tissue, as demonstrated in this study, reflects dynamic immune remodeling within the tumor microenvironment, which may occur earlier in disease progression than structural changes detectable by imaging [33]. Combining chemokine signatures with conventional markers or integrating them into multi-omic biomarker panels could enhance diagnostic accuracy, enable better risk stratification, and improve surveillance strategies in high-risk populations [34]. Furthermore, longitudinal measurement of CXCL9/10 levels might provide insights into tumor recurrence, therapeutic response, or immune reactivation following treatment, underscoring their translational potential as dynamic, immunologically informative biomarkers.

The immunosuppressive tumor microenvironment (TME) remains one of the major barriers to effective HCC therapy, contributing to poor responses to immune checkpoint inhibitors (ICIs) and rapid disease progression in many patients [35]. Strategies aimed at remodeling the TME to restore effective anti-tumor immunity are therefore of growing interest. Modulation of IL-10 signaling represents one such approach. Therapeutic delivery of recombinant IL-10 or engineered IL-10 agonists, such as pegilodecakin, has shown promise in enhancing $CD8^+$ T-cell proliferation, promoting IFN-γ production, and improving tumor control in preclinical HCC models and early-phase clinical trials [29, 36]. Combination therapies incorporating IL-10 with PD-1/PD-L1 blockade or anti-VEGF agents are under investigation and may overcome current resistance mechanisms by simultaneously alleviating immunosuppression and enhancing effector T-cell function [37].

Targeting CXCR3 signaling also offers a promising approach to disrupt tumor-promoting chemokine activity and enhance immunotherapy efficacy. Small-molecule antagonists such as AMG487 and SCH546738 have been shown to inhibit CXCR3–ligand interactions, reduce immune cell exhaustion, and suppress tumor growth in preclinical cancer models [38-40]. In addition, monoclonal antibodies directed against CXCR3 or its ligands (CXCL9/CXCL10) are being explored as adjuncts to checkpoint blockade, where they have demonstrated synergistic anti-tumor effects in experimental settings. Although still largely preclinical, these strategies highlight the translational potential of CXCR3-targeted therapies in hepatocellular carcinoma.

5. LIMITATIONS AND FUTURE DIRECTIONS

This study is limited by reliance on FPKM values rather than absolute counts, which may affect quantification accuracy. The focused panel of thirteen cytokines omits other potentially relevant mediators such as IL-17 or CCL5. Additionally, *in silico* findings require validation through orthogonal methods (quantitative PCR [qPCR], ELISA) and mechanistic studies *in vitro* or *in vivo*. Sample heterogeneity, including differences in underlying liver cirrhosis, viral status, and prior treatments, was not controlled, potentially confounding cytokine expression patterns.

Future research should prioritize integrating these transcriptomic findings with proteomic and spatial analyses to better understand cytokine dynamics within the tumor microenvironment. Larger cohorts and single-

cell RNA-seq data will be valuable for dissecting cell-type–specific contributions to cytokine regulation, while spatial transcriptomics could help map chemokine gradients and immune infiltration patterns. Moreover, longitudinal profiling of cytokine signatures during therapy could identify dynamic biomarkers predictive of treatment response or resistance.

Finally, preclinical evaluation of IL-10–based interventions and CXCR3-targeted therapies in relevant HCC models will be essential to determine their translational potential. Combining cytokine-modulating approaches with existing immunotherapies and precision-medicine strategies may offer new avenues for improving clinical outcomes in hepatocellular carcinoma.

CONCLUSION

Our study reveals a novel chemokine-driven cytokine signature in hepatocellular carcinoma, characterized by CXCL9 and CXCL10 upregulation alongside IL-10 downregulation, which collectively shape immune cell recruitment and inflammatory dynamics within the tumor microenvironment. These alterations not only underscore the immunological mechanisms underlying HCC progression but also highlight their potential utility as tissue biomarkers for early detection, prognosis, and patient stratification. Furthermore, the therapeutic modulation of IL-10 signaling and CXCR3 pathways represents a promising strategy to restore immune balance and enhance the efficacy of existing treatments. Future studies should focus on validating these findings in larger patient cohorts and exploring their clinical applicability through preclinical and translational research.

AUTHOR'S CONTRIBUTIONS

The author confirms sole responsibility for the following: study conception and design, data collection, analysis and interpretation of results, and manuscript preparation.

LIST OF ABBREVIATIONS

HCC	=	Hepatocellular Carcinoma
IL	=	Interleukin
TNF	=	Tumor Necrosis Factor
IFN	=	Interferon
CXCL	=	C-X-C Motif Chemokine Ligand
CCL	=	C-C Motif Chemokine Ligand
TGFB1	=	Transforming Growth Factor Beta 1
FPKM	=	Fragments Per Kilobase of transcript per Million mapped reads
GEO	=	Gene Expression Omnibus
RNA-seq	=	RNA Sequencing
PCA	=	Principal Component Analysis
PC	=	Principal Component
Z-score	=	Standard Score (used for data normalization)
$\log_2$(FPKM+1)	=	Log base 2 transformation of FPKM values with a pseudocount of 1
IFNG	=	Interferon Gamma
IFNA1	=	Interferon Alpha 1
IFNB1	=	Interferon Beta 1

ETHICS APPROVAL AND CONSENT TO PARTICIPATE

This study is a purely *in silico* analysis based exclusively on previously published, anonymized, and publicly available transcriptomic data obtained from the GEO database. Therefore, ethical approval was not required for this study.

HUMAN AND ANIMAL RIGHTS

Not applicable.

CONSENT FOR PUBLICATION

Not applicable.

STANDARDS OF REPORTING

STROBE guidelines were followed.

AVAILABILITY OF DATA AND MATERIALS

The data supporting the findings of this article are publicly available in the NCBI Gene Expression Omnibus (GEO) repository at https://www.ncbi.nlm.nih.gov/geo/ under accession number GSE124535. All analyses were performed using this publicly available dataset.

FUNDING

None.

CONFLICT OF INTEREST

The authors declare no conflict of interest, financial or otherwise.

ACKNOWLEDGEMENTS

The author thanks the creators of the GSE124535 dataset for making their data publicly accessible. Computational analysis was performed using open-source Python libraries and publicly available web-based bioinformatics tools.

REFERENCES

[1] Bray F, Laversanne M, Sung H, *et al*. Global cancer statistics 2022: GLOBOCAN estimates of incidence and mortality worldwide for 36 cancers in 185 countries. CA Cancer J Clin 2024; 74(3): 229-63. http://dx.doi.org/10.3322/caac.21834 PMID: 38572751

[2] El-Serag HB. Hepatocellular carcinoma. N Engl J Med 2011; 365(12): 1118-27. http://dx.doi.org/10.1056/NEJMra1001683 PMID: 21992124

[3] Finn RS, Zhu AX. Evolution of systemic therapy for hepatocellular carcinoma. Hepatology 2021; 73(S1): 150-7. http://dx.doi.org/10.1002/hep.31306 PMID: 32380571

[4] Sakurai T, Yada N, Hagiwara S, *et al*. Gankyrin induces STAT 3

activation in tumor microenvironment and sorafenib resistance in hepatocellular carcinoma. Cancer Sci 2017; 108(10): 1996-2003. http://dx.doi.org/10.1111/cas.13341 PMID: 28777492

[5] He G, Karin M. NF-κB and STAT3 – key players in liver inflammation and cancer. Cell Res 2011; 21(1): 159-68. http://dx.doi.org/10.1038/cr.2010.183 PMID: 21187858

[6] Li MO, Wan YY, Sanjabi S, Robertson AKL, Flavell RA. Transforming growth factor-β regulation of immune responses. Annu Rev Immunol 2006; 24(1): 99-146. http://dx.doi.org/10.1146/annurev.immunol.24.021605.090737 PMID: 16551245

[7] Han SH, Ju MH, Pak MG. Prognostic and therapeutic potential of CXCR6 expression on CD8 + T cells in gastric cancer: A retrospective cohort study. BMC Gastroenterol 2025; 25(1): 139. http://dx.doi.org/10.1186/s12876-025-03735-z PMID: 40050760

[8] Li L, Zhu YH, Li Y, Guan XY. Identification of chemokine CXCL10 as a prognostic marker in hepatocellular carcinoma. Neoplasma 2017; 64(5): 778-86. http://dx.doi.org/10.4149/neo_2017_517 PMID: 28592115

[9] Zhang Q, Liu L, Gong C, *et al*. Prognostic significance of tumor-associated macrophages in solid tumor: A meta-analysis of the literature. PLoS One 2012; 7(12): 50946. http://dx.doi.org/10.1371/journal.pone.0050946 PMID: 23284651

[10] Wang J, Zhang C, Chen X, *et al*. Functions of CXC chemokines as biomarkers and potential therapeutic targets in the hepatocellular carcinoma microenvironment. Transl Cancer Res 2021; 10(5): 2169-87. http://dx.doi.org/10.21037/tcr-21-127 PMID: 35116536

[11] Chiang DY, Villanueva A, Hoshida Y, *et al*. Focal gains of VEGFA and molecular classification of hepatocellular carcinoma. Cancer Res 2008; 68(16): 6779-88. http://dx.doi.org/10.1158/0008-5472.CAN-08-0742 PMID: 18701503

[12] Barrett T, Wilhite SE, Ledoux P, *et al*. NCBI GEO: Archive for functional genomics data sets-update. Nucleic Acids Res 2012; 41(D1): D991-5. http://dx.doi.org/10.1093/nar/gks1193 PMID: 23193258

[13] Ashburner M, Ball CA, Blake JA, *et al*. Gene Ontology: Tool for the unification of biology. Nat Genet 2000; 25(1): 25-9. http://dx.doi.org/10.1038/75556 PMID: 10802651

[14] Virtanen P, Gommers R, Oliphant TE, *et al*. SciPy 1.0: Fundamental algorithms for scientific computing in Python. Nat Methods 2020; 17(3): 261-72. http://dx.doi.org/10.1038/s41592-019-0686-2 PMID: 32015543

[15] Pedregosa F, Varoquaux G, Gramfort A. Scikit-learn: Machine learning in Python. J Mach Learn Res 2011; 12: 2825-30. http://dx.doi.org/10.48550/arXiv.1201.0490

[16] Tokunaga R, Zhang W, Naseem M, *et al*. CXCL9, CXCL10, CXCL11/CXCR3 axis for immune activation – A target for novel cancer therapy. Cancer Treat Rev 2018; 63: 40-7. http://dx.doi.org/10.1016/j.ctrv.2017.11.007 PMID: 29207310

[17] Wang P, Xu MH, Xu WX, Dong ZY, Shen YH, Qin WZ. CXCL9 overexpression predicts better HCC response to anti-PD-1 therapy and promotes N1 polarization of neutrophils. J Hepatocell Carcinoma 2024; 11: 787-800. http://dx.doi.org/10.2147/JHC.S450468 PMID: 38737384

[18] Aguilar-Cazares D, Chavez-Dominguez R, Marroquin-Muciño M, *et al*. The systemic-level repercussions of cancer-associated inflammation mediators produced in the tumor microenvironment. Front Endocrinol 2022; 13: 929572. http://dx.doi.org/10.3389/fendo.2022.929572 PMID: 36072935

[19] House IG, Savas P, Lai J, *et al*. Macrophage-derived CXCL9 and CXCL10 are required for antitumor immune responses following immune checkpoint blockade. Clin Cancer Res 2020; 26(2): 487-504. http://dx.doi.org/10.1158/1078-0432.CCR-19-1868 PMID: 31636098

[20] Brandt EF, Baues M, Wirtz TH, *et al*. Chemokine CXCL10 modulates the tumor microenvironment of fibrosis-associated hepatocellular carcinoma. Int J Mol Sci 2022; 23(15): 8112. http://dx.doi.org/10.3390/ijms23158112 PMID: 35897689

[21] Hsieh CH, Chuang PC, Liu YW. Beyond adaptive immunity: Trained innate immune responses as a novel frontier in hepatocellular carcinoma therapy. Cancers 2025; 17(7): 1250. http://dx.doi.org/10.3390/cancers17071250 PMID: 40227782

[22] Wang X, Zhang Y, Wang S, *et al*. The role of CXCR3 and its ligands in cancer. Front Oncol 2022; 12: 1022688. http://dx.doi.org/10.3389/fonc.2022.1022688 PMID: 36479091

[23] Nazari A, Ahmadi Z, Hassanshahi G, *et al*. Effective treatments for bladder cancer affecting the CXCL9/CXCL10/CXCL11/CXCR3 axis: A review. Oman Med J 2020; 35(2): 103. http://dx.doi.org/10.5001/omj.2020.21 PMID: 32181005

[24] Chamseddine S, Mohamed YI, Lee SS, *et al*. Clinical and prognostic biomarker value of blood-circulating inflammatory cytokines in hepatocellular carcinoma. Oncology 2023; 101(11): 730-7. http://dx.doi.org/10.1159/000531870 PMID: 37467732

[25] Xiao W, Huang H, Zheng P, *et al*. The CXCL10/CXCR3 pathway contributes to the synergy of thermal ablation and PD-1 blockade therapy. Cancers 2023; 15(5): 1427. http://dx.doi.org/10.3390/cancers15051427 PMID: 36900218

[26] Kwilasz AJ, Grace PM, Serbedzija P, Maier SF, Watkins LR. The therapeutic potential of interleukin-10 in neuroimmune diseases. Neuropharmacology 2015; 96(Pt A): 55-69. http://dx.doi.org/10.1016/j.neuropharm.2014.10.020 PMID: 25446571

[27] Saraiva M, O'Garra A. The regulation of IL-10 production by immune cells. Nat Rev Immunol 2010; 10(3): 170-81. http://dx.doi.org/10.1038/nri2711 PMID: 20154735

[28] Neumann C, Scheffold A, Rutz S. Functions and regulation of T cell-derived interleukin-10. Semin Immunol 2019; 44: 101344. http://dx.doi.org/10.1016/j.smim.2019.101344 PMID: 31727465

[29] Ouyang W, Rutz S, Crellin NK, Valdez PA, Hymowitz SG. Regulation and functions of the IL-10 family of cytokines in inflammation and disease. Annu Rev Immunol 2011; 29(1): 71-109. http://dx.doi.org/10.1146/annurev-immunol-031210-101312 PMID: 21166540

[30] Tannir NM, Papadopoulos KP, Wong DJ. Pegilodecakin Phase I study in renal cell carcinoma. Int J Cancer 2021; 149(2): 403-8. http://dx.doi.org/10.1002/ijc.33556 PMID: 33709428

[31] Salkeni MA, Naing A. Interleukin-10 in cancer immunotherapy: From bench to bedside. Trends Cancer 2023; 9(9): 716-25. http://dx.doi.org/10.1016/j.trecan.2023.05.003 PMID: 37321942

[32] Farinati F, Marino D, De Giorgio M, *et al*. Diagnostic and prognostic role of alpha-fetoprotein in hepatocellular carcinoma: Both or neither? Am J Gastroenterol 2006; 101(3): 524-32. http://dx.doi.org/10.1111/j.1572-0241.2006.00443.x PMID: 16542289

[33] Lok AS, Sterling RK, Everhart JE. DCP and AFP as biomarkers for early detection of hepatocellular carcinoma. Gastroenterology 2010; 138(2): 493-502. http://dx.doi.org/10.1053/j.gastro.2009.10.031 PMID: 19852963

[34] Maravelia P, Silva DN, Rovesti G, *et al*. Liquid biopsy in hepatocellular carcinoma: Opportunities and challenges. Cancers 2021; 13(17): 4334. http://dx.doi.org/10.3390/cancers13174334 PMID: 34503144

[35] Bicer F, Kure C, Ozluk AA, El-Rayes BF, Akce M. Advances in immunotherapy for hepatocellular carcinoma. Curr Oncol 2023; 30(11): 9789-812. http://dx.doi.org/10.3390/curroncol30110711 PMID: 37999131

[36] Jin H, Qin S, He J, *et al*. New insights into checkpoint inhibitor immunotherapy and its combined therapies in hepatocellular carcinoma: From mechanisms to clinical trials. Int J Biol Sci 2022; 18(7): 2775-94. http://dx.doi.org/10.7150/ijbs.70691 PMID: 35541908

[37] Lee HW, Cho KJ, Park JY. Current status and future direction of immunotherapy in hepatocellular carcinoma. Immune Netw 2020; 20(1): 11. http://dx.doi.org/10.4110/in.2020.20.e11 PMID: 32158599

[38] Groom JR, Luster AD. CXCR3 ligands: Redundant, collaborative and antagonistic functions. Immunol Cell Biol 2011; 89(2): 207-15. http://dx.doi.org/10.1038/icb.2010.158 PMID: 21221121

[39] Huo R, Jiang Y, Zhang L, Du S, Zhou D. CXCR3 inhibitors for therapeutic interventions: Current status and perspectives. Front Pharmacol 2025; 16: 1556196. http://dx.doi.org/10.3389/fphar.2025.1556196 PMID: 40786052

[40] Jenh CH, Cox MA, Cui L, *et al*. A selective and potent CXCR3 antagonist SCH 546738 attenuates the development of autoimmune diseases and delays graft rejection. BMC Immunol 2012; 13(1): 2. http://dx.doi.org/10.1186/1471-2172-13-2 PMID: 22233170